

STRESS CORROSION CRACKING OF PRESTRESSING STEEL IN SULPHIDE MEDIUM

NS RENGASWAMY, K S RAJAGOPALAN, K I VASU

Central Electrochemical Research Institute, Karaikudi - 623 006

and B V RANGANATHAM

Dept. of Civil Engineering, Indian Institute of Science, Bangalore

ABSTRACT

Stress corrosion cracking behaviour of cold-drawn and stress-relieved prestressing steel of standard quality conforming to I.S. 1785 - Part I has been studied in H_2S saturated aqueous solution with and without chloride. The steel was found to be highly susceptible to cracking even under open circuit condition at room temperature. The susceptibility decreased slightly with temperature in the range $30^\circ C - 80^\circ C$. The threshold stress was found to increase with pH of the medium from 15% of proof stress at pH 2.6 to 40% of proof stress at pH 6.5. A limiting pH of 7 above which stress corrosion cracking did not occur was obtained for water - H_2S system and the corresponding value in 3.5% NaCl - H_2S system was found to be 9. Cathodic polarisation decreased the time to failure while anodic polarisation increased the time to failure. Application of tensile stress was found to increase the corrosion rate and also the solubility of hydrogen. The strain rate was found to have profound influence on the cracking process and the susceptibility was high at very low strain rates. SEM fractographic studies revealed that the fracture mode was predominantly intergranular. All these observations could be understood in terms of a decohesion model.

Key Words: Stress Corrosion Cracking, Prestressing steel; Hydrogen permeation

INTRODUCTION

Many strategic structures like bridges, pressure vessels, storage tanks, piles, poles, railway sleepers and nuclear reactor protective shells are of prestressed concrete in which the prestressing steel is in permanent state of tension to compensate for the inadequate tensile strength of concrete. The prestressing steel is four to six times stronger than mild steel and such high strength steels are susceptible to stress corrosion cracking in a variety of environments especially in sulphide medium.

Earlier work indicates that steels with hardness levels exceeding $R_c 20$ corresponding to yield strength of approximately $620 N/mm^2$ exhibit susceptibility in sulphide medium [1]. Water must be present for sulphide cracking to occur, since ionisation is necessary for the liberation of hydrogen from H_2S [2]. The time to failure increases as the concentration of H_2S is reduced [3]. In general, failure did not occur at pH values above 9 [4]. However, cold-drawn wires can crack at pH values as high as 12 [5]. Available data indicate that cracking resistance increases with temperature [6]. A temperature limit exists above which steels are not susceptible to sulphide cracking. Additions of acetic acid, cyanides, CO_2 , chlorides etc. to aqueous H_2S solutions are reported to increase the cracking severity [8-10]. Cold working has a detrimental effect by increasing the hydrogen solubility and by creating residual stresses [7]. Cracking resistance is significantly reduced by manganese and chromium [11]. There is no apparent correlation between fracture toughness and resistance to sulphide cracking [4].

The common occurrence of sulphide cracking failures of many steels in the intergranular mode led to the study of the grain boundary [6]. Auger electron spectroscopy of the fractured surface indicated that S and Mn precipitated in the form of a thin film of (Fe, Mn)S. Carbon is an efficient trap for hydrogen and the high interaction energy between carbon and hydrogen can lead to the occurrence of high local concentrations of hydrogen in grain boundaries [11]. Micro auto radiography of tritium observed through SEM or TEM was used to locate hydrogen trapped in the microstructure of 7-9.4% Cr steel after cathodic charging. Many investigators have observed transgranular cracking [8].

Above literature information indicates that high strength steels as a class are readily susceptible to sulphide cracking. In fact, several instances of prestressing wire failures in concrete structures in Germany have been attributed to hydrogen sulphide released by reaction of carbon dioxide and moisture with sulphides in cement [12]. Aluminous cements in particular contain calcium sulphide. In 1957, 247 heat treated prestressing rods out of a total of 252 broke during construction of a concrete highway bridge in Brazil within 10 days of tensioning [13]. The failure was traced to liberation of hydrogen sulphide from a mixture of sulfur, lampblack, kaolin and motor oil used during construction. Sulphur reacted with hydrocarbons in oil to produce hydrogen sulphide.

Failures of prestressed concrete cowsheds, made with a special high alumina cement incorporating blast furnace slag, have been reported [14] after three years. The corrosion product contained iron sulphide. Hydrogen sulphide evolved by the action of CO_2 on the CaS in the moist humid atmosphere had embrittled the wire. Instances of embrittlement by sulphides have also been reported [15-17].

Critical examination of the literature review has revealed that excepting some work carried out by Gilchrist and Narayan [18] on the influence of microstructures, no detailed studies have so far been carried out on the mechanism of cracking of prestressing steel in sulphide medium. This work is thus concerned with stress corrosion cracking behaviour of cold-drawn and stress-relieved prestressing steel in sulphide medium. Studies were first conducted on specificity of hydrogen and sulphide ions. Then the threshold values for both stress and pH were established. Effect of temperature was also studied to see whether the process is thermally activated or otherwise. This was followed by electrochemical studies on E_{corr} and i_{corr} to understand the role of stress on corrosion behaviour. The effect of H_2S on the mechanical properties and the role of stress on hydrogen permeation were finally investigated to comprehend the actual failure mechanism. Examination of fractographs was made to identify crack morphology.

EXPERIMENTAL

The material used was 7 mm nominal diameter, single high-tensile, cold-

drawn and stress-relieved wire of standard quality conforming to IS:1785-Part I (equivalent to BS:2961 and ASTM Designation A82-62T). The chemical composition of the material is given in Table-I and the mechanical properties are given in Table-II. The specimen configuration used in the experiments is shown in fig. 1. The specimens before use were abraded with 1/0, 2/0, 3/0 and 4/0 emeries and degreased with trichloroethylene.

Table-I: Chemical composition of the prestressing steel

% C	% Mn	% Si	% Cr	% S	% P
0.85	0.80	0.27	0.29	0.04	0.02

Table-II: Mechanical properties

Ultimate tensile stress (N/mm ²)	...	1700
Proof stress at 0.2% elongation (N/mm ²)	...	1500
Breaking stress (N/mm ²)	...	1200
Elongation % on gauge length of 30 mm	...	3.3
Rockwell hardness	...	C43

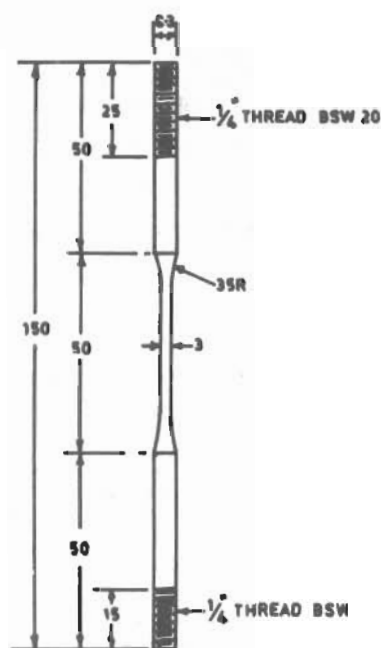


Fig. 1: High tensile steel specimen for stress corrosion studies

As the prestressing steel wire in practice is permanently held in a state of uniaxial tension, it was decided to adopt constant load test for SCC studies to represent the service condition. UNISTEEL stress corrosion testing machine, Mark II supplied by W.H. Mayes and Sons (Windsor) Ltd., England which had a lever loading arrangement was used for this purpose. The diagram of the constant load stress corrosion cell is shown in fig. 2. Time to failure was studied as a function of applied tensile stress, temperature, pH and polarisation.

Dynamic mechanical testing under a constant strain rate was carried out in a MONSANTO TENSOMETER 2000 of 20 KN capacity.

For electrochemical studies, a Wenking Laboratory Potentiostat Model LB75M with fast response in conjunction with a Wenking Voltage Scan Generator Model VSG 72 was used. A RIKADENKI X-Y Recorder RW101 was used to record E vs i , E vs t and i vs t .

Hydrogen permeation studies were carried out using the electrochemical method of Bockris and Devanathan [19]. The experimental set up is shown in fig. 3. The permeation membrane was made out of the

7 mm dia prestressing wire in a shaping machine. The mechanical properties were determined for this membrane in Tensometer. Two identical half cells were joined together with the permeation membrane in between with teflon

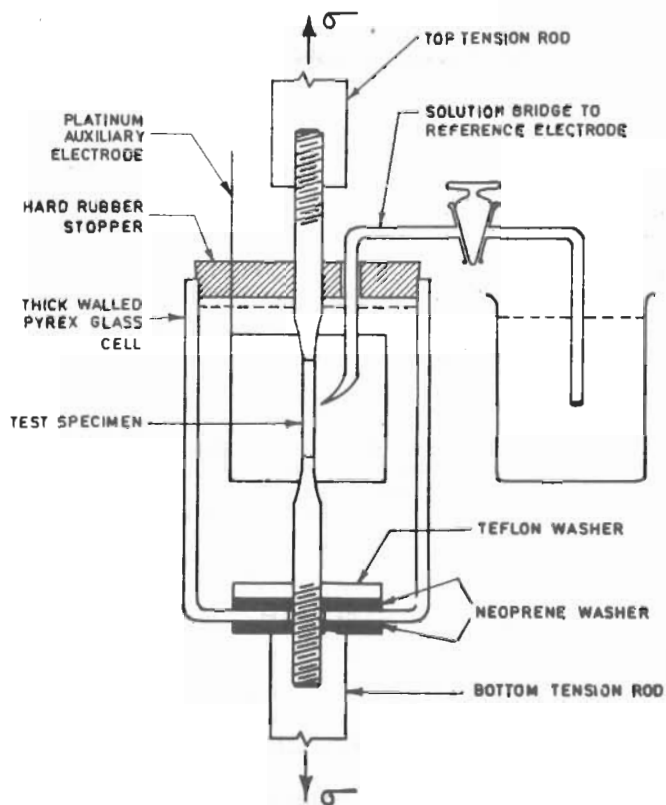


Fig. 2: Diagram of the constant load stress corrosion cell

gaskets and stainless steel flanges and bolts. Hydrogen was generated cathodically on one side of the membrane at a constant current density and the flux of hydrogen arriving on the other side was constantly oxidized and

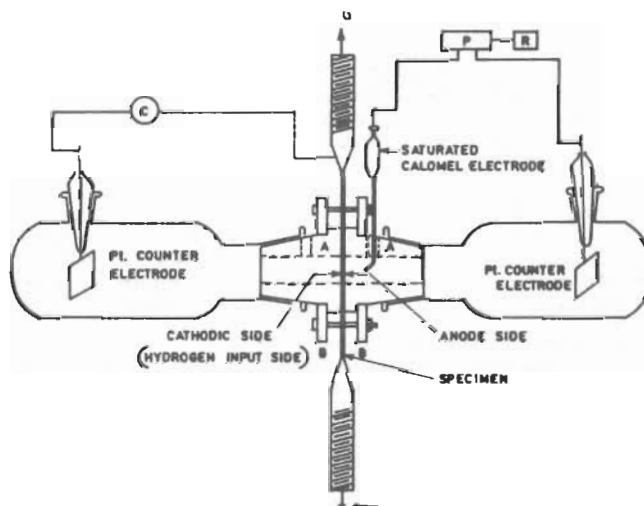


Fig. 3: Experimental cell arrangement for hydrogen permeation studies

turned into an equivalent current which was recorded as a function of time. From this permeation current-time transient, the diffusion coefficient of hydrogen and solubility of hydrogen were calculated.

Fractured specimens were examined with a Scanning Electron Microscope (JEOL, JSM 35 CF, Japan).

RESULTS AND DISCUSSION

a) Specificity of hydrogen and sulphide ions

In order to find out the specific environmental requirement for sulphide cracking, constant load tests were carried out at 90% proof stress with various combinations of solutions at room temperature and in each test the time to failure was noted. The results are reported in Table-III.

Table III: Time to failure in different media

Stress: 90% of proof stress		Temperature 303 K (30°C)
No.	Medium	Time to failure (min)
1.	Air	NF
2.	Distilled water	NF
3.	3.5% NaCl solution	NF
4.	Hydrochloric acid (pH = 2.6)	NF
5.	10% Na ₂ S	NF
6.	Distilled water saturated with H ₂ S	21
7.	3.5% NaCl soln. saturated with H ₂ S	25
8.	3.5% NaCl soln. + 0.5% acetic acid saturated with H ₂ S (pH = 2.6)	13

NF—No fracture up to 200 hours

It can be seen that cracking does not occur even in 200 hours of static loading in solutions of sodium chloride (3.5%) sodium sulphide (10%) or hydrochloric acid (pH 2.6). The cracking occurs only when the above solutions are saturated with H₂S using a Kipps apparatus. This is specifically needed for cracking to occur. Further the cracking is produced at room temperature under open circuit condition without any need for polarisation.

b) Threshold stress

The specimens were subjected to different percentages of proof stress and the time to failure was noted in each case. The results are presented in fig. 4. It

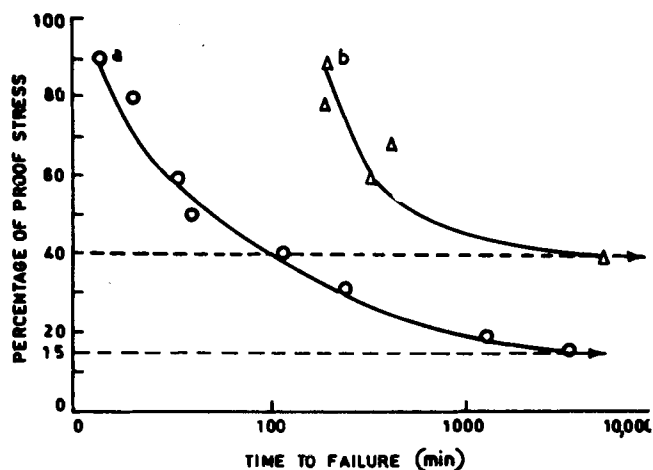


Fig. 4: Applied stress vs time to failure in

- 3.5% NaCl + 0.5% acetic acid + H₂S (saturated) (pH = 2.6) Room temperature 303 K²
- 3.5% NaCl + 0.04 N NaOH + H₂S (saturated) (pH = 6.5) Room temperature 303 K

can be seen that at a pH of 2.6, the threshold stress is around 15% of proof stress and by increasing the pH from 2.6 to 6.5, threshold stress value is increased from 15% to 40% proof stress.

c) Effect of pH

3.5% NaCl solution saturated with H₂S was taken as the base medium and the pH was adjusted either by addition of acetic acid or by sodium hydroxide. The results are shown in fig. 5.

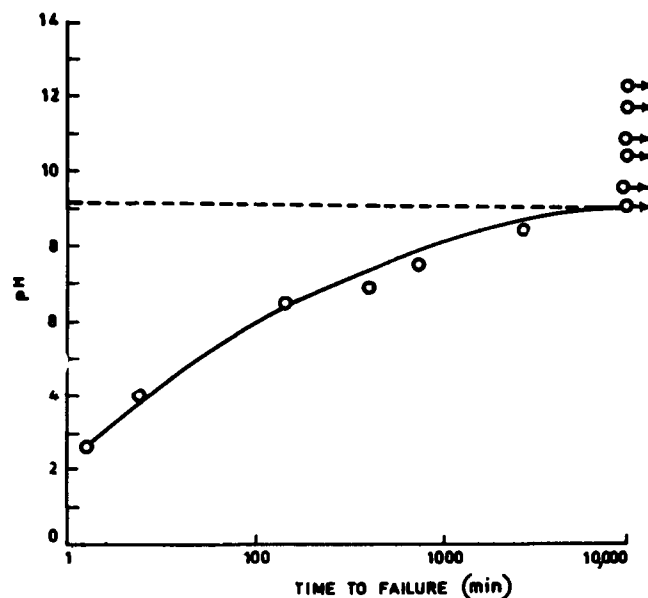


Fig. 5: pH vs time to failure in 3.5% NaCl—H₂S system, stressed to 90% of proof stress

It is seen that time to failure increases exponentially with pH and that there is a limiting pH around 9 beyond which fracture in the presence of H₂S is completely inhibited.

Similar studies were made in double distilled water saturated with H₂S. The results are given in fig. 6. In this case also, the time to failure increases exponentially with pH and the limiting pH value beyond which there is no failure is around 7.

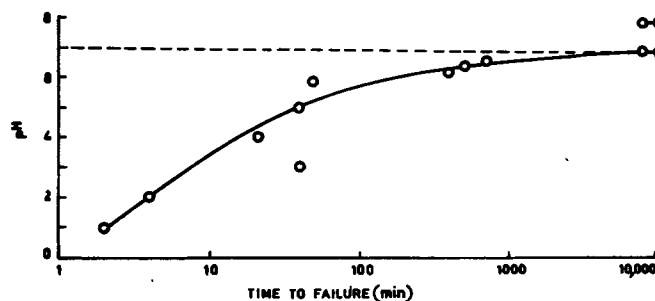


Fig. 6: pH vs time to failure in distilled water—H₂S system, stressed to 90% of proof stress

d) Effect of temperature

Effect of temperature on time to failure was studied in double distilled water saturated with H₂S (pH 4) at 90% proof stress. Temperature was maintained constant by using a water jacket around the cell and circulating constant temperature water. It is seen from fig. 7 that the temperature has relatively minor influence on time to failure. By increasing the temperature from 30°C to 80°C, time to failure gets almost linearly increased from 21 minutes to 30 minutes indicating that the process is not thermally activated.

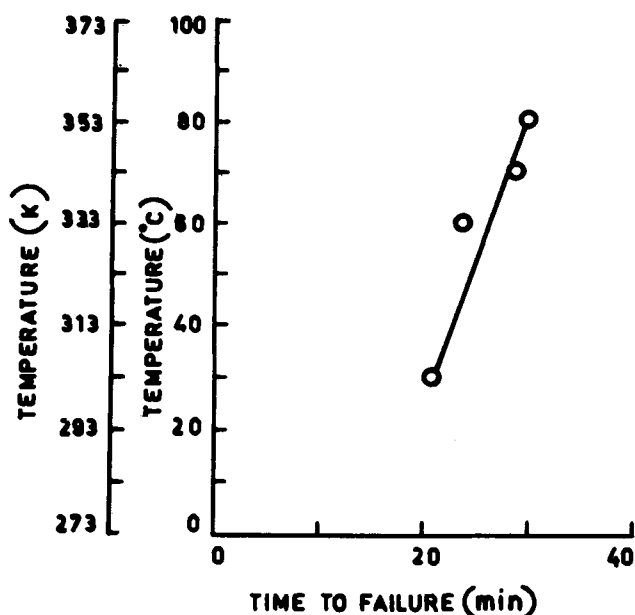


Fig. 7: Temperature vs time to fracture in double distilled water— H_2S system—stressed to 90% of proof stress

e) Potential-time studies

The variation of corrosion potential was followed with time in 3.5% NaCl + 0.5% acetic acid solution saturated with H_2S at different stress levels. Fig. 8 shows that in general, the potential moves in the more negative direction and tends to attain a steady state value of around -670 mV vs SCE. This indicates that initially corrosion increases and then attains a steady state value independent of stress.

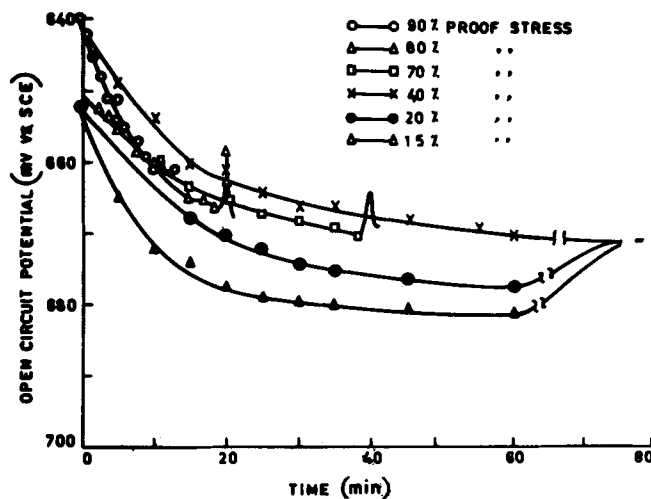


Fig. 8: Variation of corrosion potential with time in 3.5% NaCl + 0.5% acetic acid + H_2S (pH 2.6)

f) Polarisation studies

To see the influence of stress on the corrosion process, cathodic and anodic polarisation studies were made in double distilled water saturated with H_2S (pH 4) at 0% and 60% of proof stress. Corrosion current ' i_{corr} ' and corrosion potential ' E_{corr} ' were obtained by Tafel interpolation method. It is seen from

fig. 9 and Table-IV that compared with 0% stress, application of 60% proof stress increases i_{corr} from 17 to $40 \mu A/cm^2$ and shifts E_{corr} in the more negative direction.

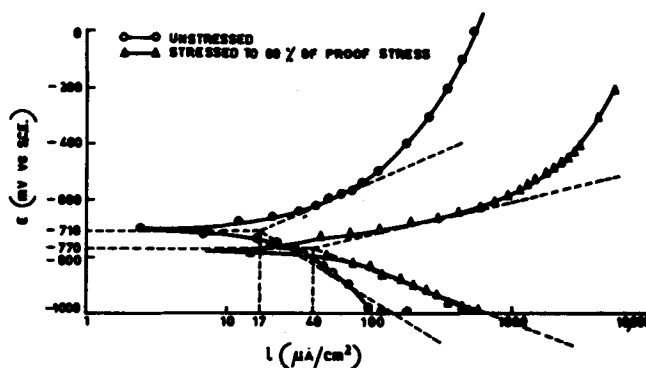


Fig. 9: Effect of stress on i_{corr} in double distilled water— H_2S system

Table IV: Effect of stress on E_{corr} and i_{corr}

Medium : Double distilled water saturated with H_2S
pH : 4.0
Temperature: 303 K (30°C)

No.	Percentage of proof stress	E_{corr} (mV vs S.C.E)	i_{corr} ($\mu A/cm^2$)
1	0	-710	17
2	60	-710	40

When the polarisation studies were carried out in 3.5% NaCl + 0.5% acetic acid saturated with H_2S solution (pH 2.6), stress was found to have no significant effect on i_{corr} and E_{corr} as can be seen from Table-V. This is in conformity with the inference drawn from potential-time studies.

Table V: Effect of stress on E_{corr} and i_{corr}

Medium : 3.5% NaCl + 0.5% acetic acid + H_2S
pH : 2.6
Temperature: 303 K (30°C)

No.	Percentage of proof stress	E_{corr} (mV vs S.C.E)	i_{corr} ($\mu A/cm^2$)
1	0	-660	2000
2	40	-650	2100
3	50	-650	2000

g) Potentiostatic studies

The specimen was exposed to 3.5% NaCl + 0.5% acetic acid saturated with H_2S solution (pH 2.6) and stressed to 40% of stress. Each specimen was held at different constant potentials and the time to failure was noted. It is observed from fig. 10 that the time to failure decreases as the potential of the specimen is shifted in the cathodic direction. There appears a critical cathodic potential around 130 mV. Up to an overpotential of 130 mV, the time to failure decreases steeply and then remains constant indicating that the rate controlling mechanism attains a steady state at this potential. Anodic polarisation on the other hand is found to increase the time to failure. This study thus indicates that cathodic charging of hydrogen atoms brings about accelerated failure.

h) Effect of strain rate

The dissolved hydrogen in metal can produce severe damage to the metal causing considerable decrease in strength and ductility. To see the effect

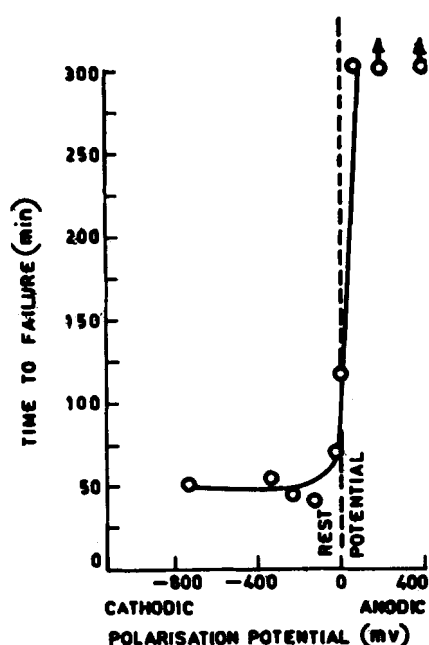


Fig. 10: Time to failure vs polarisation potential in 3.5% NaCl + 0.5% acetic acid + H₂S, stressed to 40% of proof stress

produced by hydrogen on the mechanical properties, tests were conducted in MONSANTO Tensometer under different strain rates with the specimen kept immersed in a medium of 3.5% NaCl + 0.5% acetic acid + H₂S (pH 2.6) during the test. The results are presented in Table-VI and fig. 11.

Table VI: Effect of strain rate on mechanical properties

a) Testing in H₂S medium
Medium : 3.5% NaCl + 0.5% HAc + H₂S
pH : 2.6
Temperature : 303 K (30°C)

No.	Strain rate ($\times 10^{-3}$ /S)	UTS (N/mm ²)	RA (%)
1	0.33	1670	5.23
2	0.66	1715	12.87
3	1.65	1670	23.76
4	3.3	1685	27.16
5	6.6	1735	34.94
6	9.9	1675	37.06
7	16.5	1685	42.29
8	33.0	1695	44.27

b) Testing in air

1	0.33	1750	40.0
2	0.66	1670	43.0
3	1.65	1670	38.0
4	6.6	1755	39.0
5	16.5	1760	37.0
6	33.0	1730	45.0

For comparison, the results of the tests conducted in air are also included. It is seen that in presence of the H₂S medium, only the percentage reduction in area is significantly affected. The ultimate tensile strength is not appreciably

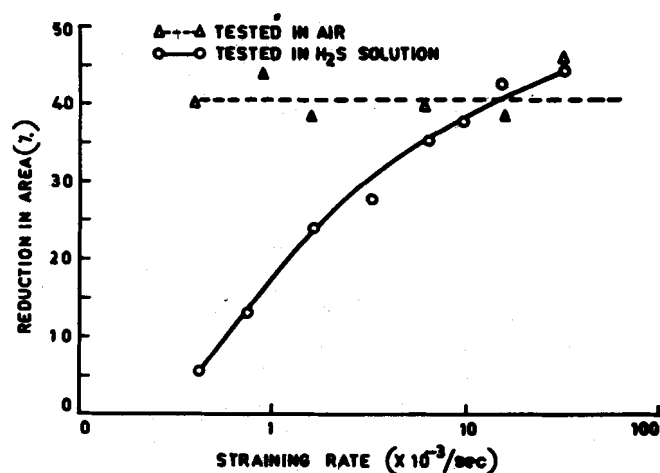


Fig. 11: Effect of straining rate on reduction in area of section in 3.5% NaCl + 0.5% acetic acid + H₂S (pH = 2.6)

affected. This study shows that the strain rate has profound influence on the cracking process and at very slow strain rates, the susceptibility is high.

i) Hydrogen permeation studies

0.4 and 0.5 mm thick membranes were prepared out of 7 mm dia. prestressing steel, abraded to 4/0 finish, annealed, degreased and used in the studies. From the experimental values of steady state permeation current 'J' and half rise transient 'T_{1/2}', diffusion coefficient 'D' and solubility of hydrogen C₀ were calculated [20]. The results are presented in Table VII.

Table VII: Hydrogen permeation studies-Effect of applied tensile stress

i) Thickness 0.04 cm, Cathodic current 50 mA/cm²

Applied stress (% proof stress)	J (μ A/cm ²)	T _{1/2} (sec.)	D ($\times 10^{-6}$)	C ₀ (gm atom/ cc $\times 10^{-6}$)
0	5	294	0.8	2.6
50	6	294	0.8	3.1

ii) Thickness 0.05 cm, cathodic current 100 mA/cm²

Applied stress (% proof stress)	J (μ A/cm ²)	T _{1/2} (sec.)	D ($\times 10^{-6}$)	C ₀ (gm atom/ cc $\times 10^{-6}$)
0	1.8	60	5.8	0.16
50	2.7	60	5.8	0.24
75	3.6	60	5.8	0.32

It is seen that the application of tensile stress increases the permeation current as well as the solubility of hydrogen. This is in conformity with the observation made by Beck et al [21] on 4340 steel that the diffusion coefficient of stress and only the solubility was affected by stress.

j) Fractography

Samples which were fractured in media of different pH were first observed. Samples fractured under slow straining rate and fast straining rate were also observed for existence of different mechanism.

Fig. 12 shows the fractured surface of a specimen fractured in a H₂S medium of pH 2.6 at 90% proof stress. Major portion is of intergranular type, but dimpled rupture is also identified. Perhaps the final portion of the fast fracture was ductile. In this case the time to fracture was shortest.

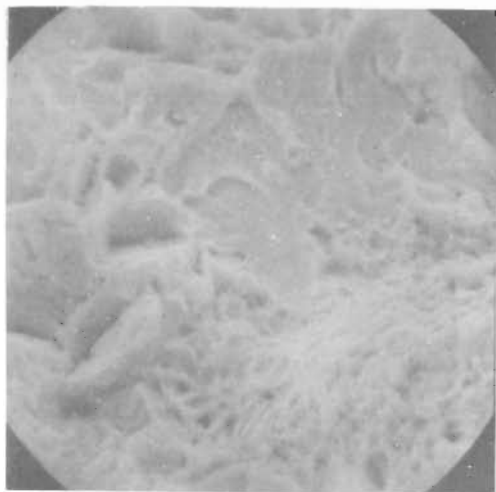


Fig. 12: SEM Fractograph of specimen fractured in 3.5% NaCl + 0.5% acetic acid + H_2S (pH = 2.6), 90% proof stress



Fig. 13: SEM Fractograph of specimen fractured in 3.5% NaCl + 0.5% acetic acid + H_2S (pH = 2.6), 40% proof stress

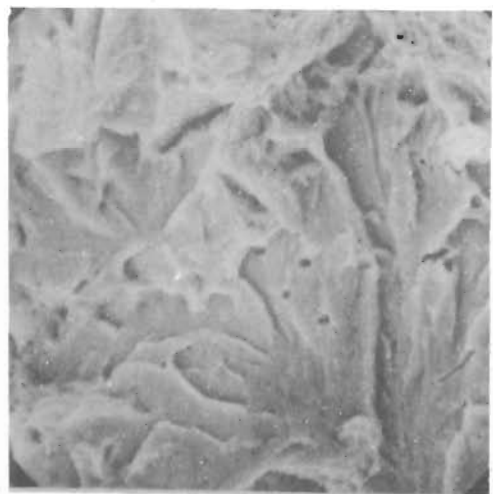


Fig. 14: SEM Fractograph of specimen fractured in double distilled water + H_2S (pH = 4), 90% proof stress

At 40% proof stress in the same medium where the time to failure was more, the fracture as observed in fig. 13 is predominantly intergranular with some cleavage facets.

When the medium is free of chloride i.e. double distilled water saturated with H_2S (pH 4) cleavage facets are observed (Fig. 14).

When the pH is increased to alkaline side, corrosion protection is more predominant and secondary cracks are observed (Fig. 15). The mode is intergranular with easily identifiable grain boundary facets. Cathodic charging in the same medium, leads to mixed type of fracture as was observed in pH 2.6 (Fig. 16).

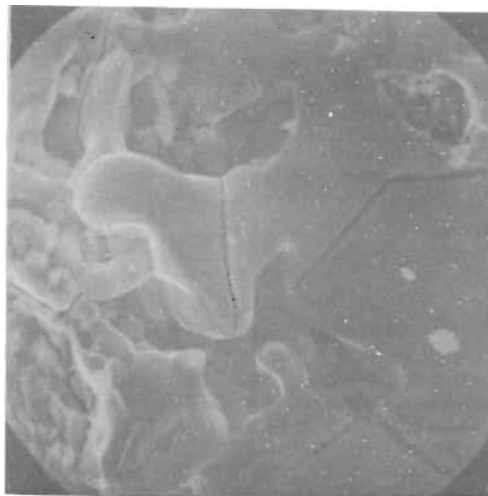


Fig. 15: SEM Fractograph of specimen fractured in 0.1N NaOH + 3.5% NaCl + H_2S (pH = 8.5), 90% proof stress

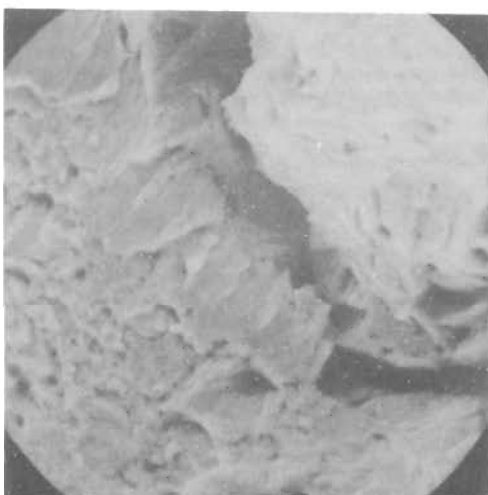


Fig. 16: SEM Fractograph of specimen fractured in 0.1N NaOH + 3.5% NaCl + H_2S (pH = 8.5), 90% proof stress, cathodic potential 1000 mV

Fig. 17 shows fractographs of samples fractured under slow strain rate. Tear ridges and globular inclusions are identified. Under fast strain rate, a mixed mode of dimple fracture + intergranular fracture is observed (Fig. 18).

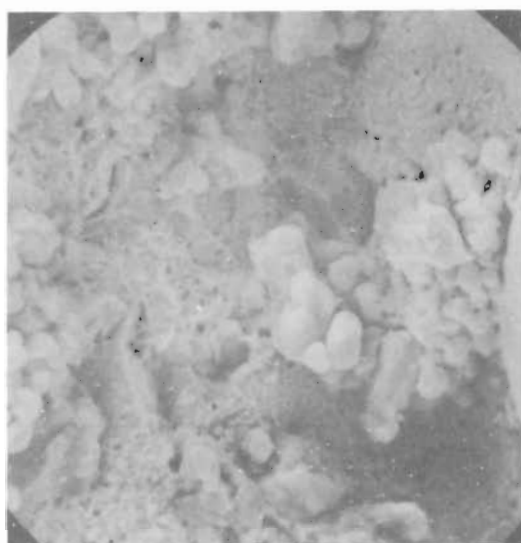


Fig. 17: SEM Fractograph of specimen fractured under slow strain rate in 3.5% NaCl + 0.5% acetic acid + H₂S (pH = 2.6)



Fig. 18: SEM Fractograph of specimen fractured under fast strain rate in 3.5% NaCl + 0.5% acetic acid + H₂S (pH = 2.6)

From the above observations, it may be broadly concluded that the failure mode is mixed type but predominantly intergranular.

CRACKING MECHANISM

The recombination of atomic hydrogen is generally inhibited by the presence of sulphides [22]. H₂S poisons the surface available for the recombination of atomic hydrogen and thus promotes its entry into the steel. Hydrogen adsorption is the important factor influencing cracking of steel in hydrogen sulphide solutions. Acetate ions stimulate hydrogen adsorption while chloride ions inhibit [23].

Solution pH has a significant effect on sulphide cracking susceptibility. The corrosion rate in H₂S solutions is influenced by the nature of the film formed on the steel surface [24]. The increase in corrosion rate with a decrease in pH is due to a decrease in the protective properties of the surface

film. As the pH increases, threshold stress also increases. This shows that stress has a very important role in the cracking mechanism and as a more protective surface film is formed at high pHs, more stress is required to weaken the film and bring about the cracking.

A study of the time to fracture at different potentials reveals that time to failure decreases considerably even at very low cathodic overpotential while time to failure increases quite appreciably at low anodic overpotential. This only shows that as more hydrogen is produced at the surface, because of the concentration gradient, more atomic hydrogen is able to get into the metal and cause the fracture.

Studies on the effect of temperature has shown that the process is not thermally activated. From the hydrogen permeation studies, it is observed that the application of tensile stress results in increased hydrogen solubility.

Since ultimate strength of the material is not affected in this system, formation of brittle hydride phase is not a possibility. Pressure theory is to be discounted on the fact that the crack propagation is so fast in this system studied at room temperature and atmospheric pressure that there is no time and favourable conditions for build up of pressure inside.

In a highly cold worked metal like the one used in this study, edge dislocation energy decreases and climb is easy. Hydrogen can seriously affect the cohesiveness of such metals by interaction with the dislocation network. The diffusing hydrogen has to interact with a highly stressed region. Decohesion therefore seems to be the more appropriate rate-controlling mechanism. High strength steel of this type has a large number of highly elastically stressed regions and thus there exists a thermodynamic motivation for large accumulation of dissolved hydrogen and this atomic hydrogen concentrates at the point of maximum triaxial stress and decreases the cohesive strength at that point and brings about fracture at lower nominal stresses.

The mechanism thus involves the cracking of FeS film, the liberation of hydrogen at the crack tip, its absorption and stress-induced diffusion leading to accumulation at weak grain boundaries consequently resulting in cracking by decohesion.

CONCLUSION

The cold drawn and stress-relieved prestressing steel is highly susceptible to cracking in H₂S medium, the susceptibility slightly decreasing with temperature. The threshold stress is very low and it is found to increase with pH of the medium from 15% of proof stress at pH 2.6 to 40% of proof stress at pH 6.5.

A limiting pH of 7 above which stress corrosion cracking did not occur was obtained for water H₂S system and the corresponding value in 3.5% NaCl-H₂S system was found to be 9.

The fracture mode is predominantly intergranular. The mechanism appears to be one of hydrogen embrittlement by decohesion along grain boundaries.

REFERENCES

1. EH Phelps, Proc. Conf. 'Fundamental Aspects of Stress Corrosion Cracking' edited by R W Staehle, A J Forty and D Van Rooyen (1969) p 398
2. R S Treseder and T M Swanson, *Corrosion* **24** (1968) 31
3. P G Bastein, 'Physical Metallurgy of Stress Corrosion Fracture' edited by Thor N Rhodin, Interscience Publishers Inc. New York (1959)
4. H Inshi Zuka and K Onishi, *J. Jap. Inst. Metals* **30** (1966) 846
5. E Shape, *Corrosion*, **11** (1967) 154
6. DR Johnston and T G Mc Cord, *Proc. NACE 26th Conf.* (1970)
7. FK Bloom, *Corrosion*, **11** (1955) 351 t
8. J P Fraser and R S Treseder, *Corrosion*, **8** (1952) 342
9. J P Fraser, G G Eldridge and R S Treseder, *Corrosion* **14** (1958) 517 t

10. HR Copson, *Weld. J.* **32** (1953) 759
11. RM Hudson and GI Strangand, *Corrosion* **16** (1960) 253 t
12. DG Moore, DT Kloot and RJ Hansen, *Protection of steel in prestressed concrete bridges*, National Cooperative Highway Research Station, Program Report 90, Highway Research Board, National Academy of Science (1970)
13. W Grundig, An Inter American Approach for the seventies, Materials Technology, *J. Am. Soc. Mech. Engg* (1970) 508
14. FK Naumann and A Baumel, Archive, Eisenhüttenwesen, **32-2** (1961) 65
15. GR Spare, *Wire. Wire. Prod.* **28** (1954) 1421
16. RL McGlasson and WD Greathouse, *Corrosion*, **14** (198) 517 t
17. VR Thayer, *Eng News-Rec.* **29-3** (1962) 8
18. JD Gilchrist and R Narayan, *Corrosion Sci.* **11** (1971) 281
19. J O'M Bockris and MA V Devanathan, ONR Technical Report 551, 22 (1957)
20. J McBreen and L Nanis, *J Electrochem Soc* **113** (1966) 1218
21. W Beck, J O'M Bockris, J McBreen and L Nanis, *Proc. Roy. Soc.* **A90** (1966) 220
22. G V Karpenko and II Vasilenko, 'Stress Corrosion Cracking of steels, Freund Publishing House, Tel Aviv, Israel (1979)
23. JP Fraser, GG Eldrige and RS Treseder, *Corrosion* **14** (1958) 517 t
24. J Sardisco and R Pitts, *Corrosion* **21** (1965) 245